

Enhanced therapeutic effects of Mesenchymal Stem Cell-derived Extracellular Vesicles within Chitosan Hydrogel in the treatment of Diabetic Foot Ulcers

Shuangshuang Yang (✉ shuangshuang0323@126.com)

Qilu Cell Therapy Technology Co., Ltd

Siyu Chen

Qilu Cell Therapy Technology Co., Ltd

Chunyuan Lin

Qilu Cell Therapy Technology Co., Ltd

Xiaohui Zhao

Qilu Cell Therapy Technology Co.,Ltd

Yi Tan

Qilu Cell Therapy Technology Co., Ltd

Research Article

Keywords: Mesenchymal stem cells, Extracellular vesicles, Chitosan hydrogel, Diabetic foot ulcers, Cell-free therapy

Posted Date: June 1st, 2022

DOI: <https://doi.org/10.21203/rs.3.rs-1663280/v1>

License:   This work is licensed under a Creative Commons Attribution 4.0 International License.

[Read Full License](#)

Abstract

Background: Extracellular vesicles (EVs) derived from human umbilical cord mesenchymal stem cells (UC-MSCs) have emerged as promising cell-free therapy candidates in various diseases, including chronic cutaneous wounds. The goal of this study was to create a safe and efficient method for large-scale production of MSC-derived EVs and establish an EVs identification protocol to advance the clinical application of EVs in wound therapy.

Methods: Polyethylene glycol (PEG) precipitation and ultracentrifugation were used to isolate EVs from the culture supernatant of UC-MSCs. Transmission electron microscopy (TEM), Western blot, and a high-sensitivity flow cytometer (HSFCM) were used to examine the size distribution, particle concentration, and phenotype of EVs. Chitosan hydrogel-EVs were created to improve the use of EVs in wound treatment by incorporating EVs into chitosan hydrogel (CS-EVs). The Transwell method was used to assess the release behavior and uptake dynamics of EVs from chitosan hydrogel in vitro. The scratch wound assay and tube formation assay were used to determine whether EVs altered the migration and angiogenesis of human umbilical vein endothelial cells (HUVECs). Every five days, CS-EVs were transplanted onto the wound site of a diabetic rat model. On days 0, 5, 10, and 20 following surgery, wound healing processes were graphically recorded and evaluated. Finally, after 15 days of surgery, all rats were sacrificed, and the wound skin was collected for hematoxylin and eosin (H&E) staining.

Results: The majority of the EVs obtained in our protocol had a cup-shaped or round-shaped morphology with a diameter of about 80 nm. CD9, CD63, and CD81 were all found. In the experiment, the chitosan hydrogel was liquid at 4 °C and was gelatinized for 10 minutes at 37 °C. The CS-EVs continuously released EVs into the environment, and the EVs released by the CS-EVs were internalized by human umbilical vein endothelial cells (HUVECs), resulting in significant cell migration and angiogenesis promotion. Furthermore, we discovered that CS-EVs have a good therapeutic function in the promotion of wound healing in a rat model of diabetic foot ulcers.

Conclusions: Our findings suggest that PEG precipitation and ultracentrifugation can be used to isolate EVs on a large scale. Chitosan hydrogel-EVs (CS-EVs) were formed by incorporating EVs into chitosan hydrogels, which is an effective application scheme for EVs in wound therapy. Overall, our research could help with the purification, characterization, and application of EVs in wound care.

1. Introduction

Diabetes mellitus is a lifelong metabolic disease characterized by chronic hyperglycemia. It is caused by multiple etiologies. Due to the high mortality and morbidity, the disease has now become a serious health problem worldwide. With an increase in the aging population and changes in dietary structure, the incidence of diabetes has continued to rise in recent years [1, 2]. Diabetes can trigger various complications and endanger the heart, brain, kidneys, peripheral nerves, eyes, feet, and other organs. Diabetic foot ulcer (DFU) is a serious and complex complication of diabetes [3, 4], and its pathologies

include diabetic neuropathy, peripheral vascular disease, and ulceration. Multiple factors, including infection, hyperglycemia, and impaired angiogenesis, may result in delayed or even non-healing of the ulcer wound [5, 6]. The treatment of DFU mainly includes controlling blood sugar, local debridement, and wound treatment. Unfortunately, no effective solution is available to promote the healing of complex wounds yet [7].

Recently, several studies have shown that mesenchymal stem cells (MSCs) contribute to angiogenesis, acceleration of epithelial regeneration, improvement of granulation formation, and promotion of chronic wound closure by secreting cytokines, chemokines, and growth factors, etc. [8–11]. The usage of MSCs in DFU therapy has provided a promising regenerative therapeutic modality [12]. However, MSCs cannot survive for a long time in the wound tissue and usually disappear within 24 h, which poses a challenge for their application in wound treatment [13]. Additionally, ambiguous effects of MSCs transplantation, including potential tumorigenicity and undesired immune responses, remain a concern while using MSCs in DFU therapy [14].

Extracellular vesicles (EVs) released from living cells are essential for intercellular communication. EVs transport functional molecules over long distances while affecting the behavior of cells by delivering a variety of substances, including proteins, mRNAs, and microRNAs, to recipient cells [15]. EVs exhibit commendable beneficial functions similar to their parental cells [16, 17]. MSC-derived EVs are considered functional mediators of MSCs, which exert immune regulation and promote regeneration [18, 19]. Notably, MSC-derived EVs also show a lower propensity in triggering an immune response [20]. Considering the safety in clinical applications, EVs may have specific advantages compared to stem cell therapy. However, recovering damaged tissue is a complex multi-stage process, and due to the action of the immune system, it is inevitable for free EVs to get rapidly cleared off the system [21]. Hence, another challenge in using EVs for wound treatment includes reducing their rapid clearance. Thermosensitive chitosan hydrogel is widely used as a carrier for various treatments. Cells or drugs can be incorporated into the chitosan hydrogel, a highly biocompatible polymer material, through cross-linking [22]. The cross-linked chitosan hydrogel can then release cells or drugs slowly into the system, increasing the *in situ* retention time of the loaded substances [23]. This suggests that the incorporation of EVs within chitosan hydrogel can reduce the rapid clearance of EVs, providing their enhanced beneficial effects on the recovery of wound tissues.

In our study, we established an efficient protocol to isolate and characterize MSC-derived EVs, where the EVs were combined with chitosan hydrogel to form CS-EVs, making them more effective for wound treatment. We also evaluated the beneficial effects of CS-EVs in endothelial cells and a rat model of diabetic foot ulcers. Our data suggested that the incorporation of EVs within the chitosan hydrogel represented a novel approach for maintaining the therapeutic efficacy of MSCs-derived EVs in accelerating deficient skin healing.

2. Materials And Methods

2.1 Cell culture

The umbilical cord from full-term neonates delivered abdominally was collected in sterile condition. Mesenchymal stem cells (MSCs) were obtained by enzyme digestion and cultured in Dulbecco's Modified Eagle Medium (DMEM)/F12 medium. The MSCs (Passages 3–6) were expanded using (DMEM)/F12 medium with 10% bovine fetal bovine serum (FBS) and 100 U/mL penicillin-streptomycin. Human umbilical vein endothelial cells (HUVECs) were purchased from ATCC (Manassas, VA) and cultured using Dulbecco's Modified Eagle Medium (DMEM) containing 10% FBS and 100 U/mL penicillin-streptomycin. The basal medium, FBS, and phosphate-buffered saline (PBS) used in cell culture experiments were obtained from Gibco (Grand Island, USA) and were ultracentrifuged before use at 160 000 g for 8 h to remove vesicle analogs.

2.2 Characterization of umbilical cord-MSCs (UC-MSCs)

To assess the surface antigen of umbilical cord-MSCs (UC-MSCs), flow cytometry analysis was performed. The MSCs were first incubated with PE-conjugated antibodies against CD90, CD105, CD34, and CD45 for 20 min and then collected after centrifugation for 5 min at 1000 g. The cells were washed twice with PBS and finally resuspended in PBS for flow cytometry analysis (BD Biosciences, USA). All antibodies used in our experiment were purchased from BD Biosciences.

2.3 Multidirectional identification of UC-MSCs

The UC-MSCs (Passage 6) were seeded in 6-well plates and cultured in an appropriate differentiation medium according to the manufacturer's instructions. For adipogenic differentiation, the entire process lasted 14 days. After differentiation, the cells were stained with oil red O. Osteogenic differentiated cells were stained with alizarin red on day 21, while the chondrogenic differentiated cells were stained with alcian blue and safranin O on day 21, separately [24]. All reagents were obtained from StemCell Technologies.

2.4 Enrichment of MSC-derived extracellular vesicles

To isolate EVs, a large amount of culture medium was required, which was collected by seeding MSCs at a density of 8000 cells/cm² in the Cell Factory System. Once the cells reached 80–90% confluency, the existing medium was collected [25] and stored at – 80°C, which was pooled together to make up a volume of 6 L. The collected medium was then centrifuged at 16 000 g for 30 min at 4°C to remove the whole cells and excess cellular debris. To enrich the EVs in the supernatant, we used the description of Rider et al. [26] with slight modifications and added PEG 6000 to the medium to achieve a final PEG concentration of 8%. Samples were mixed thoroughly and incubated for 12 h at 4°C. After which, the samples were centrifuged at 12 000 g for 1 h at 4°C. The resultant pellet was thoroughly dissolved in 10 mL of PBS and ultracentrifuged at 120 000 g for 60 min to obtain EVs. Later, EV solutions were stored at – 80°C for further processing.

2.5 Transmission electron microscopy (TEM)

Transmission electron microscopy (TEM) was used to observe the morphologies of EVs. EV samples were dropped onto a carbon grid and adsorbed for 20 min. Next, the EVs were fixed in 1% glutaraldehyde for 5 min, washed with PBS, and visualized using a transmission electron microscope (Hitachi, Japan) [27].

2.6 Western Blot Analysis

An equal amount of protein from both EVs and MSC samples was loaded on 12% sodium dodecyl sulfate polyacrylamide gel electrophoresis (SDS-PAGE) and transferred onto poly vinylidene fluoride (PVDF) membranes. The membranes were then incubated with primary antibodies CD9, CD63, CD81, and GM130 overnight at 4°C. Later, the membranes were developed with horseradish peroxidase-conjugated secondary antibody and visualized. The western blot results were used to analyze the expression of exosomal markers in the isolated EVs.

2.7 High-sensitivity flow cytometry analysis

To measure accurate particle concentration in high-sensitivity flow cytometry analysis (Flow NanoAnalyzer U30, NanoFCM), the EVs suspension was diluted to 1:1000 with filtered PBS. For immunofluorescence staining analysis, PE-conjugated antibodies specific to CD9, CD63, or CD81 were added to the EV suspension while to investigate the co-expression of CD9, CD63, and CD81 in individual vesicles, PE-conjugated antibodies (for CD9 and CD63) and PerCP Cy5.5-conjugated antibodies (for CD63 and CD81) were added to EV suspensions and determined using double immunization fluorescent staining analysis. All antibodies were purchased from BD Biosciences.

2.8 Preparation and Characterization of chitosan hydrogel

Chitosan hydrogel was prepared as per the previous report [28]. A stock solution of 2% chitosan was prepared by dissolving chitosan powder (Hidebei, China) in 0.1 M acetic acid. Similarly, a 50% β -glycerophosphate (β -GP) solution was prepared in sterile water. Both solutions were then sterilized by filtration and stored at 4°C until subsequent applications. For the experiment, both 50% β -GP and 2% chitosan solution were stirred in the water bath at a volume ratio of 5:1 at 37°C to form a chitosan hydrogel. Later, the EVs (1×10^{10} particles) were mixed well with 5 volumes of 2% chitosan hydrogel by stirring in an ice bath to obtain the chitosan hydrogel-incorporated EVs (CS-EVs). Finally, the parallel plate rheometer was used to measure the elastic moduli (G') and viscous moduli (G'') to investigate the rheological properties of chitosan hydrogel and CS-EVs at different temperatures ranging between 4°C and 37°C.

2.9 *In vitro* study of the release dynamics of CS-EVs

The release behavior of EVs leaching from the chitosan hydrogel *in vitro* was evaluated using the Transwell method. The chitosan hydrogel was first mixed with EVs (1×10^{11} particles) to form the CS-EVs, as mentioned above. The CS-EVs solution was then loaded onto the upper chamber of the Transwell (approximately 200 μ L per well) and mounted on a 24-well plate, followed by gelatinization for 10 min at 37°C to form CS-EVs. Next, the CS-EVs were submerged in 1.5 mL PBS at 37°C for different time points

(up to 3 days). Subsequently, the supernatants were collected for high-sensitivity flow cytometer (HSFCM) analysis to evaluate the release ratio of EVs. Meanwhile, the release behaviors of EVs at lower doses were also studied by similarly processing the chitosan hydrogel and EVs (1×10^{10} particles).

2.10 *In vitro* study of the uptake dynamics of CS-EVs

The EVs were stained with PKH26 (Sigma-Aldrich, USA) as per the manufacturer's instructions. The uptake behavior of EVs leaching from CS-EVs in HUVEC cells was further determined using the method described above. The preparation of CS-EVs (1×10^{11} particles) was similar to the above description, i.e., the CS-EV solution was loaded on the upper chamber of the Transwell, and then the HUVEC were seeded in a 24-well plate at a density of 6000 cells/cm². After 12 h, HUVECs were gently washed with PBS and fixed in 4% paraformaldehyde for 15 min. The washing step was repeated, and the cells were stained with FITC Phalloidin and DAPI (Solarbio, China). The signals from the stained cells were detected using laser scanning confocal microscopy LSM780 (Zeiss, GRE).

2.11 Migration tests

A scratch wound healing assay was performed to determine the beneficial effects of CS-EVs on the promotion of cell migration. Upon HUVECs reaching 90% confluency, a pipette tip was used to create a scratch in the confluent cell layer. Next, both chitosan hydrogel and CS-EVs (1×10^{11} particles) were loaded on the upper chamber of the Transwell, and the cells were cultured at 37°C for an additional 22 h. The migration distance of cells at 6 h and 22 h was observed under the microscope and photographed.

2.12 Tube formation assay

We performed an *in vitro* tube formation assay to test the proangiogenic effect of leached EVs. Matrigel obtained from BD Biosciences was thawed at 4°C and added to a 24-well plate (approximately 300 μ L per well). HUVECs were seeded on the Matrigel-coated plate and treated with an FBS-free medium. Next, the chitosan hydrogel and CS-EVs (1×10^{11} particles) were loaded on the upper chamber of the Transwell and incubated for 8 h. After which, images were acquired using a microscope with a camera system.

2.13 *In vivo* animal experiments

Healthy Sprague-Dawley (SD) rats, weighing 240 ± 20 g, were purchased from SPF Biotechnology Co., Ltd. For the construction of the diabetic rat model, the rats were first fed a high-sucrose and high-fat diet for 10 weeks and then administered an intraperitoneal injection of STZ (35 mg/kg, Sigma) at the 10th and 11th weeks. The criterion for successful model construction was a value of fasting blood glucose > 11 mmol/L for more than 4 weeks.

Next, we anesthetized twenty-four rats and randomly divided them into four groups of six animals. Dorsal hairs of rats were shaved to create a full-thickness wound of a 10 mm diameter. Four groups were used to evaluate CS-EVs in promoting wound healing. The wounds were then covered with hydrogel without EVs, CS-EVs (1×10^{10} particles), EVs (1×10^{10} particles), or PBS. Later, the wound was covered with gauze and

3 M Tegaderm film to prevent infection. After 5, 10, or 15 days of surgery, the wound area was photographed, and the dressing was changed in every group. Finally, all rats were sacrificed after 15 days of surgery, and the skin of the wound was collected for hematoxylin and eosin (H&E) staining.

2.14 Statistical analysis

All experiments were performed in triplicates and also repeated three times at least. The SPSS 18.0 software was used for statistical analysis. Data were represented as mean \pm SD, where $P < 0.05$ was considered significant.

3. Results

3.1 Phenotypes of MSCs and multidirectional identification

Our results demonstrated a typical spindle-like morphology of UC-MSCs *in vitro* (Fig. 1A). The MSCs positively expressed CD90 (96.8%) and CD105 (99.1%) but negatively expressed CD45 (0.695%) and CD34 (0.171%) (Fig. 1B). CD90 and CD105 are well known-markers of MSCs, while CD34 and CD45 are typical markers of hematopoietic stem cells. Moreover, MSCs possessed adipogenic, osteogenic, and chondrogenic differentiation abilities (Fig. 1C). Therefore, our results indicated that the MSCs were qualified for culturing and collecting conditioned medium for EVs isolation.

3.2 Isolation and Characterization of EVs

To enrich EVs, we set up a combination of PEG and ultracentrifugation. Several different techniques were also used in combination to assess the concentration, quality, morphology, and subtypes of EVs. The majority of EVs obtained in our protocol exhibited a cup-shaped or round-shaped morphology (Fig. 2A). To assess the particle concentration and size distribution of EVs isolated from the supernatants of MSCs according to our protocol, we conducted an HSFCM analysis. The nanoFCM assay results showed that the concentration of EVs was approximately averaged to $(3.97 \pm 0.044) \times 10^{11}$ particles/mL. Simultaneously, the size distribution of particles was also evaluated, and the nanoFCM data for the MSC-derived EVs indicated the average size of these particles to be 80 nm (Fig. 2B). Western blot analysis showed that EVs isolated from the supernatants of MSCs contained exosomal markers CD9, CD63, and CD81. Although GM130 was found to be highly expressed in parental cells, it was barely detectable in EVs (Fig. 2C). The subpopulation analysis of EVs was performed using the fluorescence mode of nanoFCM, and the results showed that the percentages of CD9, CD63, or CD81 positive EVs were 37.5%, 38.6%, and 19.8%, respectively (Fig. 2D). Similarly, the subpopulations of EVs co-expressing CD9/CD63, CD9/CD81, and CD63/CD81 were 26.5%, 13.7%, and 17%, respectively (Fig. 2E).

3.3 Characterization of the chitosan hydrogel

Previous studies have reported that the thermosensitive chitosan hydrogel is an ideal biocompatible polymer material, which is widely used as a carrier to deliver cells and drugs [28]. In the experiment, the

chitosan hydrogel was liquid at 4°C, which was gelatinized at 37°C for 10 min (Fig. 3A). The rheological properties of chitosan hydrogel and CS-EVs were analyzed, and the results showed that the addition of EVs did not affect the formation of the chitosan hydrogel (Fig. 3B, C).

3.4 Release and uptake behavior of EVs leaching from chitosan hydrogel

The release behavior of EVs from hydrogel to the PBS solution is shown in Fig. 4A. Our results showed that within 48 h, CS-EVs released EVs to the surroundings in a sustained manner. Both doses of EVs were released rapidly from the hydrogel within the first day. The group containing 1×10^{11} and 1×10^{10} extracellular vesicles particles showed a 24 h release rate of $78.5 \pm 3.6\%$ and $75.6 \pm 4.1\%$, respectively (Fig. 4B). Moreover, the EVs leaching from the chitosan hydrogel fused with HUVEC cells (Fig. 4C, D).

3.5 Proangiogenic capacity of CS-EVs

In vitro wound-healing assay showed an enhanced migratory capacity of HUVECs after 6 and 22 h of CS-EVs addition (Fig. 5A, B). After incubating CS-EVs for 22 h, the wound closure rate (85.7%) in the cells became significantly higher than the ones incubated with only chitosan hydrogel (57.2%) (Fig. 5C). The tube formation assays conducted to investigate the proangiogenic potential of CS-EVs showed a significant difference in the tube length and branch point values after incubation with CS-EVs compared to that of the control (Fig. 6B).

3.6 *In vivo* evaluation of the closure of a full-thickness wound

We studied a full-thickness skin wound on the back of our rat model to explore the pro-angiogenesis and wound healing effects of CS-EVs *in vivo*. Figure 7A shows the wound healing on days 0, 5, 10, and 15 in each group. At every time point, the best wound healing performance was shown by the CS-EVs group, followed by the EVs group and the chitosan hydrogel group. The PBS group performed the worst. On day 10, the wounds in each group showed different degrees of healing. After 15 days of treatment, almost no obvious scar was observed in the CS-EVs group. However, the other groups, especially the PBS group, still showed obvious scabs (Fig. 7B). On day 15, H&E staining showed that the skin tissue in the CS-EVs group was almost healed with mature glandular tissue, highly organized collagen fibers, and a dermis similar to the normal skin tissue. Compared to the other groups, CS-EVs significantly promoted the rapid healing of wounds through wound epithelization and tissue remodeling (Fig. 7C).

4. Discussion

A diabetic foot ulcer is a complex and incurable chronic wound that seriously threatens the physical and mental health of patients. Developing an effective solution to promote wound repair in diabetic patients has become an important and urgent need. Although EVs have shown therapeutic value in the DFU

model, unfortunately, no clinical trials have been conducted on them. Hence, before allowing MSC-EVs for human application, several clinical challenges and potential limitations need to be addressed [29, 18]. The lack of standardized preparation procedures and identification protocols, along with the unclear proportions of each EV subpopulation based on different isolation methods, have often led to inconsistent results. Therefore, we aimed to employ a method that enriches EVs rapidly and inexpensively from the media using polyethylene glycol, which was followed by ultracentrifugation for further purification. Simultaneously, we also identified the size distribution, particle concentration, and phenotype of extracellular vesicles using TEM, western blotting, and HSFCM analysis, respectively.

Importantly, we focused on the purity of EV preparations, especially the development of EVs for therapeutics. The purity of EVs is a major issue and a critical factor in ensuring the sensitivity and accuracy of downstream assays. Notably, the ensemble western blot analysis of CD9, CD63, and CD81 in EV preparations was not sufficient for claiming purity and recovery of EVs. Since HSFCM could be used to detect single immunostained EVs, we used bivariate fluorescence versus SSC to determine the percentages of EVs positive for CD9, CD63, or CD81. The single-particle phenotype of HSFCM holds a distinct advantage since it can quantify the number and proportion of positive particles.

EVs are nanoscale lipid bilayer vesicles released from their source cells, which can deliver cargo molecules to recipient cells for intercellular communication [30, 31]. Many studies have reported the improvement in the therapeutic capacity of EVs by modulating the microenvironment and genetically manipulating the donor cells to increase the content of beneficial proteins and functional microRNAs [32, 33]. Although cell modification is a promising strategy to improve the composition of EVs' therapeutics, it includes potential risks [34]. Furthermore, EV-induced recovery exhibits a dose-dependent pattern; for instance, increasing the dose regimen can enhance the tissue regeneration effect of EVs. However, a multiple-dose regimen requires a large amount of EVs, which increases the treatment cost and unanticipated adverse reactions.

Chitosan hydrogel was used to construct an immune isolation barrier to protect EVs from getting cleared by the host immune system. Chitosan hydrogel is reported to be a good carrier for EVs since it enhances its efficacy in the treatment of hindlimb ischemia [28]. Additionally, since chitosan hydrogel can maintain a moist wound environment and cool the wound surface, it has attracted great attention in the treatment of wounds. In this study, we focused on improving the therapeutic capacity of EVs by preventing their clearance and degradation upon administration at the wound site. To achieve this, we cross-linked EVs with chitosan hydrogel to retain them *in situ* for a longer time. With the permeation and biodegradation of chitosan hydrogel, the EVs are released with prolonged residence time and sustained delivery. Considering umbilical vein endothelial cells as the research object, Transwell experiments were conducted to confirm the release of EVs from chitosan hydrogel for internalization by cells, promotion of migration, and angiogenesis. Also, the strategy of combining EVs with chitosan showed significantly better results in animal experiments compared to using EVs alone.

However, our study had some limitations. First, there was a lack of functional component analysis of EVs and the exploration of their mechanism of action for wound repair. Second, since the release of EVs in this study relied on the penetration and degradation of chitosan hydrogel, the process was difficult to control. Therefore, the pore size and biodegradability of chitosan hydrogel needed optimization. In the future, designing and synthesizing a novel hydrogel loaded with spatiotemporal molecular signals for the precise and controllable release of EVs may be required to enhance the therapeutic capabilities of EVs.

5. Conclusions

In summary, we developed a safe and effective method to mass-produce MSC-derived EVs. EVs were incorporated into chitosan hydrogel to better understand the application of EVs in wound treatment to form chitosan hydrogel-EVs (CS-EVs). The CS-EVs could release EVs to the surroundings in a sustained manner. Moreover, the EVs released from the CS-EVs could be readily internalized by HUVECs and significantly promote their migration and angiogenesis *in vitro* conditions. Additionally, CS-EVs significantly improved wound recovery rate in the rat model of diabetic foot ulcers. Overall, our study may provide solutions for the purification, characterization, and application of EVs in wound treatment.

Abbreviations

EVs
Extracellular vesicles
UC-MSCs
Umbilical cord mesenchymal stem cells
PEG
Polyethylene glycol
TEM
Transmission electron microscopy
HSFCM
High-sensitivity flow cytometer
CS-EVs
Chitosan hydrogel-EVs
HUVECs
Human umbilical vein endothelial cells
DFU
Diabetic foot ulcer
MSCs
Mesenchymal stem cells
DMEM
Dulbecco's Modified Eagle Medium
FBS

Fetal bovine serum
PBS
phosphate-buffered saline
 β -GP
 β -glycerophosphate
SDS-PAGE
sodium dodecyl sulfate polyacrylamide gel electrophoresis
PVDF
poly vinylidene fluoride.

Declarations

Acknowledgements

Not applicable.

Authors' contributions

SY helped with the conceptualization, methodology, and first draft writing. SC helped with data analysis, as well as reviewing, editing, and writing the manuscript. CL helped with the investigation, examination, and software. XZ helped with formal analysis, validation, supervision, and resource allocation. YT and SY are in charge of project management and funding acquisition. The final manuscript was read and approved by all authors.

Funding

Ministry of Science and Technology of China (2021YFA1101500), and Natural Science Foundation of Shandong Province, China (ZR2021QC202).

Availability of data and materials

The datasets generated during the current study are available from the figshare repository. <http://doi.org/10.6084/m9.figshare.19778791>.

Ethics approval and consent to participate

This study was approved by the Medical Ethics Committee of Qilu Hospital of Shandong University. All animal studies complied with the principles based on the International Guiding Principles for Biomedical Research Involving Animals.

Consent for publication

Not applicable.

Competing interests

The authors declare that they have no competing interests.

Author details

Qilu Cell Therapy Technology Co., Ltd, No.1758 Gangyuan Six Road, Jinan, Shandong, China

References

1. International Diabetes Federation. IDF Diabetes Atlas Ninth. Dunia: IDF; 2019.
2. Krug EG. Trends in diabetes: sounding the alarm. *Lancet*. 2016;387:1485–86.
3. Yazdanpanah L, Nasiri M, Adarvishi S. Literature review on the management of diabetic foot ulcer. *World J Diabetes*. 2015;6(1):37–53.
4. Boulton AJ, Vileikyte L, Ragnarson-Tennvall G, Apelqvist J. The global burden of diabetic foot disease. *Lancet*. 2005;366(9498):1719–24.
5. Shiekh PA, Singh A, Kumar A. Exosome laden oxygen releasing antioxidant and antibacterial cryogel wound dressing OxOBand alleviate diabetic and infectious wound healing. *Biomaterials*. 2020;249:120020.
6. Greenhalgh DG. Wound healing and diabetes mellitus. *Clin Plast Surg*. 2003;30(1):37–45.
7. Shi Q, Qian ZY, Liu DH, Sun J, Wang X, Liu HC, et al. GMSC-Derived Exosomes Combined with a Chitosan/Silk Hydrogel Sponge Accelerates Wound Healing in a Diabetic Rat Skin Defect Model. *Front Physiol*. 2017;8:904.
8. Mathew SA, Naik C, Cahill PA, Bhonde RR. Placental mesenchymal stromal cells as an alternative tool for therapeutic angiogenesis. *Cell Mol Life Sci*. 2019;77(2):253–65.
9. Gao W, Chen DW, Liu GJ, Ran XW. Autologous stem cell therapy for peripheral arterial disease: A systematic review and meta-analysis of randomized controlled trials. *Stem Cell Res Ther*. 2019;10(1):140.
10. Gu JW, Huang L, Zhang C, Wang Y, Zhang RB, Tu ZL, et al. Therapeutic evidence of umbilical cord-derived mesenchymal stem cell transplantation for cerebral palsy: A randomized, controlled trial. *Stem Cell Res Ther*. 2020;11(1):43.
11. Dalirfardouei R, Jamialahmadi K, Jafarian AH, Mahdipour E. Promising effects of exosomes isolated from menstrual blood-derived mesenchymal stem cell on wound-healing process in diabetic mouse model. *J Tissue Eng Regen Med*. 2019;13(4):555–68.
12. Huang YZ, Gou M, Da LC, Zhang WQ, Xie HQ. Mesenchymal stem cells for chronic wound healing: current status of preclinical and clinical studies. *Tissue Eng Part B Rev*. 2020;26(6):555–70.
13. Wu Y, Huang S, Enhe J, Ma K, Yang SM, Sun TZ, et al. Bone marrow-derived mesenchymal stem cell attenuates skin fibrosis development in mice. *Int Wound J*. 2014;11(6):701–10.

14. Klopp AH, Gupta A, Spaeth E, Andreeff M, Marini F. Concise review: Dissecting a discrepancy in the literature: Do mesenchymal stem cells support or suppress tumor growth? *Stem Cells*. 2011;29(1):11–9.
15. Lötvall J, Hill AF, Hochberg F, Buzás EI, Vizio DD, Gardiner C, et al. Minimal experimental requirements for definition of extracellular vesicles and their functions: A position statement from the International Society for Extracellular Vesicles. *J Extracell Vesicles*. 2014;3:26913.
16. Qi X, Zhang JY, Yuan H, Xu ZL, Li Q, Niu X, et al. Exosomes Secreted by Human-induced Pluripotent Stem Cell-derived Mesenchymal Stem Cells Repair Critical-sized Bone Defects through Enhanced Angiogenesis and Osteogenesis in Osteoporotic Rats. *Int J Biol Sci*. 2016;12(7):836–49.
17. Hu L, Wang J, Zhou X, Xiong ZH, Zhao JJ, Yu R, et al. Exosomes Derived from Human Adipose Mesenchymal Stem Cells Accelerates Cutaneous Wound Healing via Optimizing the Characteristics of Fibroblasts. *Sci Rep*. 2016;6:32993.
18. Huang C, Luo WF, Wang Q, Ye YF, Fan JH, Lin L, et al. Human Mesenchymal Stem Cells Promote Ischemic Repairment and Angiogenesis of Diabetic Foot Through Exosome miRNA-21–5p. *Stem Cell Res*. 2021;52:102235.
19. Sjöqvist S, Ishikawa T, Shimura D, Kasai Y, Imafuku A, Bou-Ghannam S, et al. Exosomes derived from clinical-grade oral mucosal epithelial cell sheets promote wound healing. *J Extracell Vesicles*. 2019;8(1):1565264.
20. Rani S, Ryan AE, Griffin MD, Ritter T. Mesenchymal Stem Cell-derived Extracellular Vesicles: Toward Cell-free Therapeutic Applications. *Mol Ther*. 2015;23(5):812–23.
21. Imai T, Takahashi Y, Nishikawa M, Kato K, Morishita M, Yamashita T, et al. Macrophage-dependent Clearance of Systemically Administered B16BL6-derived Exosomes from the Blood Circulation in Mice. *J Extracell Vesicles*. 2015;4:26238.
22. Peppas NA, Hilt JZ, Khademhosseini A, Langer R. Hydrogels in Biology and Medicine: From Molecular Principles to Bionanotechnology. *Adv Mater*. 2006;18(11):1345–60.
23. Ruel-Gariépy E, Leroux JC. In situ-forming hydrogels-review of temperature-sensitive systems. *Eur J Pharm Biopharm*. 2004;58(2):409–26.
24. Woods EJ, Perry BC, Hockema J, Jeffrey, Larson L, Zhou D, Goebel WS. Optimized cryopreservation method for human dental pulp-derived stem cells and their tissues of origin for banking and clinical use. *Cryobiology*. 2009;59(2):150–7.
25. Lee JH, Ha DH, Go HK, Youn J, Kim HK, Jin RC, et al. Reproducible Large-Scale Isolation of Exosomes from Adipose Tissue-Derived Mesenchymal Stem/Stromal Cells and Their Application in Acute Kidney Injury. *Int J Mol Sci*. 2020;21(13):4774.
26. Rider MA, Hurwitz SN, Meckes DG. ExtraPEG: A Polyethylene Glycol-Based Method for Enrichment of Extracellular Vesicles. *Sci Rep*. 2016;6:23978.
27. Théry C, Witwer KW, Aikawa E, Alcaraz MJ, Anderson JD, Andriantsitohaina R, et al. Minimal information for studies of extracellular vesicles 2018 (MISEV2018): a position statement of the

- International Society for Extracellular Vesicles and update of the MISEV2014 guidelines. *J Extracell Vesicles*. 2018;7(1):1535750.
28. Zhang KY, Zhao XN, Chen XN, Wei YZ, Du W, Wang YB, et al. Enhanced Therapeutic Effects of MSC-derived Exosomes with an Injectable Hydrogel for Hindlimb Ischemia Treatment. *Acs Appl Mater Interfaces*. 2018;10(36):30081–91.
 29. An T, Chen Y, Tu YC, Lin P. Mesenchymal Stromal Cell-Derived Extracellular Vesicles in the Treatment of Diabetic Foot Ulcers: Application and Challenges. *Stem Cell Rev Rep*. 2021;17(2):369–78.
 30. Théry C, Zitvogel L, Amigorena S. Exosomes: composition, biogenesis and function. *Nat Rev Immunol*. 2002;2(8):569–79.
 31. Valadi H, Ekström K, Bossios A, Sjöstrand M, Lee JJ, Lötvall JO. Exosome-mediated transfer of mRNAs and microRNAs is a novel mechanism of genetic exchange between cells. *Nat Cell Biol*. 2007;9(6):654–9.
 32. Lopatina T, Bruno S, Tetta C, Kalinina N, Porta M, Camussi G. Platelet-derived growth factor regulates the secretion of extracellular vesicles by adipose mesenchymal stem cells and enhances their angiogenic potential. *Cell Commun Signal*. 2014;12:26.
 33. Xin HQ, Li Y, Liu ZW, Wang XL, Shang X, Cui YS, et al. MiR-133b promotes neural plasticity and functional recovery after treatment of stroke with multipotent mesenchymal stromal cells in rats via transfer of exosome-enriched extracellular particles. *Stem Cells*. 2013;31(12):2737–46.
 34. Armstrong JPK, Holme MN, Stevens MM. Re-Engineering Extracellular Vesicles as Smart Nanoscale Therapeutics. *ACS Nano*. 2017;11(1):69–83.

Figures

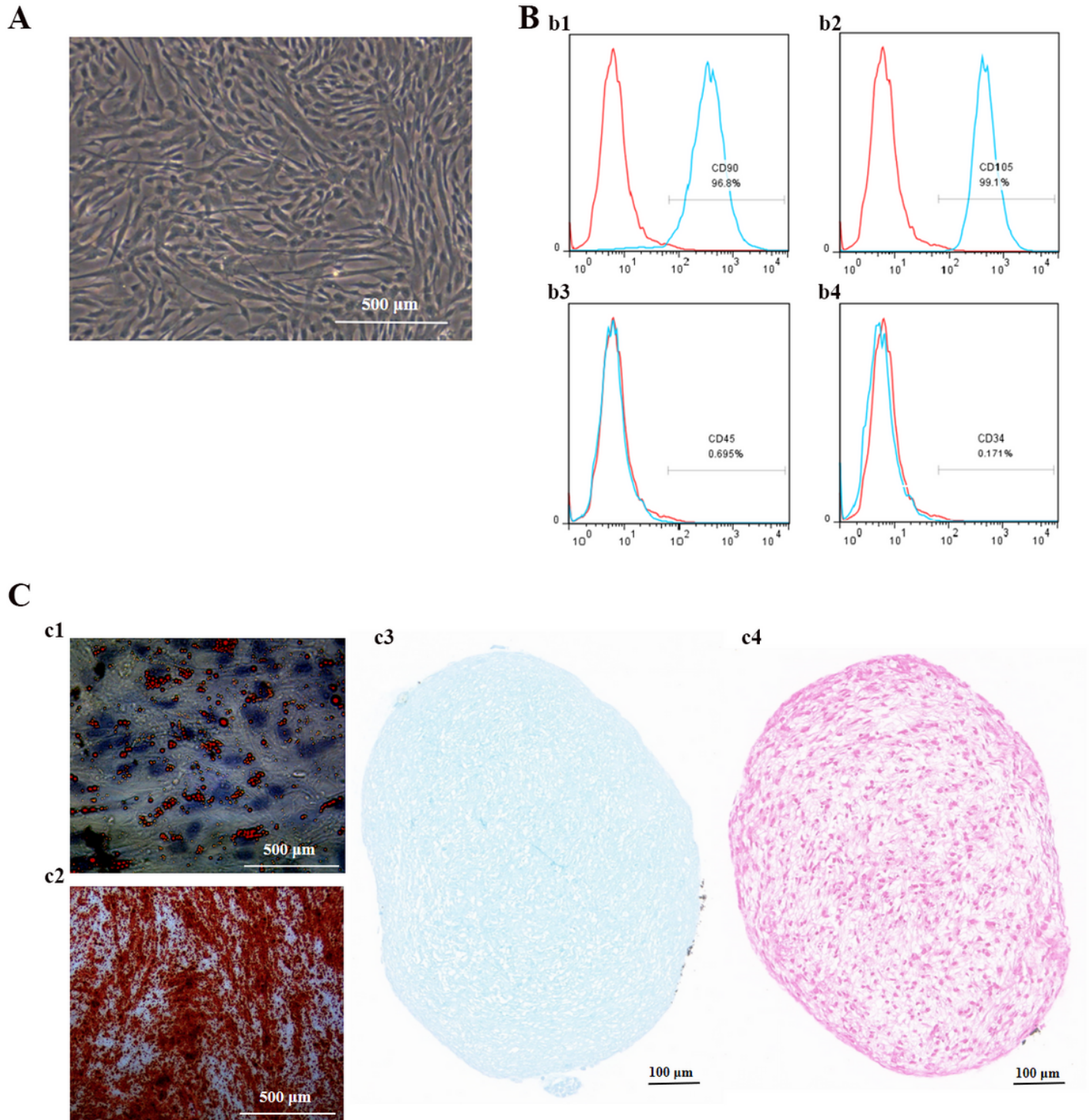


Figure 1

Characterization of UC-MSCs. **A.** Morphology of UC-MSCs. **B.** Surface markers of UC-MSCs. The cells were positive for CD90 (b1) and CD105 (b2) and negative for CD45 (b3) and CD34 (b4). **C.** The multidirectional identification of UC-MSCs; c1. Oil red staining of UC-MSCs; c2. Alizarin red staining of UC-MSCs; c3. Alcian blue staining of UC-MSCs; c4. Safranin O staining of UC-MSCs.

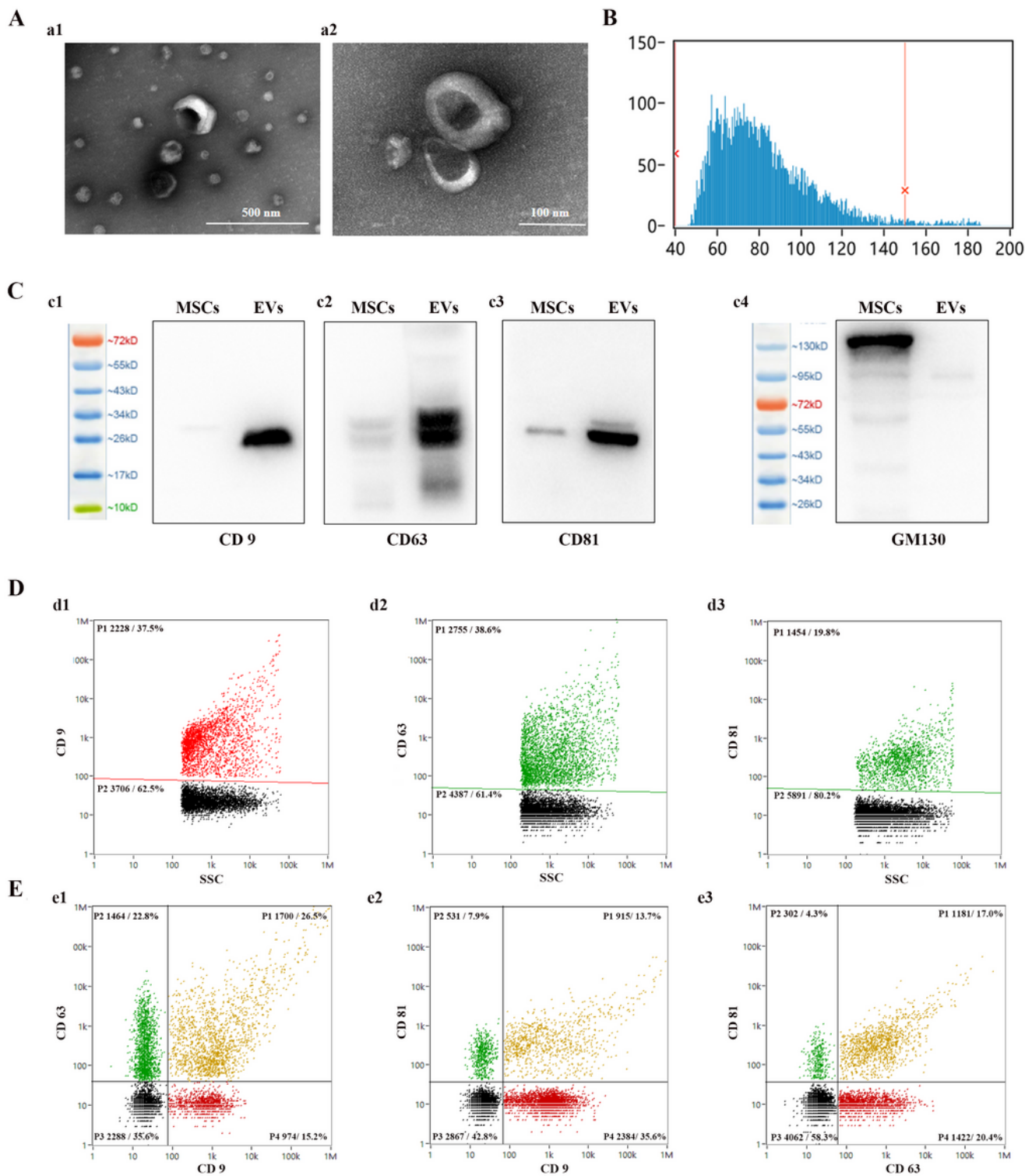


Figure 2

Characterization of MSCs-derived EVs. **A.** TEM images of EVs; Scale bar: 500 nm (a1), Scale bar: 100 nm (a2). **B.** The particle size distribution of EVs. **C.** CD9 (c1), CD63 (c2), CD81 (c3), and GM130 (c4) markers of MSCs and EVs. **D.** HSFCM analysis of CD9 (d1), CD63 (d2), and CD81 (d3) in MSCs-derived EVs. **E.** The co-expression analysis of CD9, CD63, and CD81 of EVs. Subpopulations of EVs co-expressing CD9/CD63 (e1), CD9/CD81 (e2), and CD63/CD81 (e3).

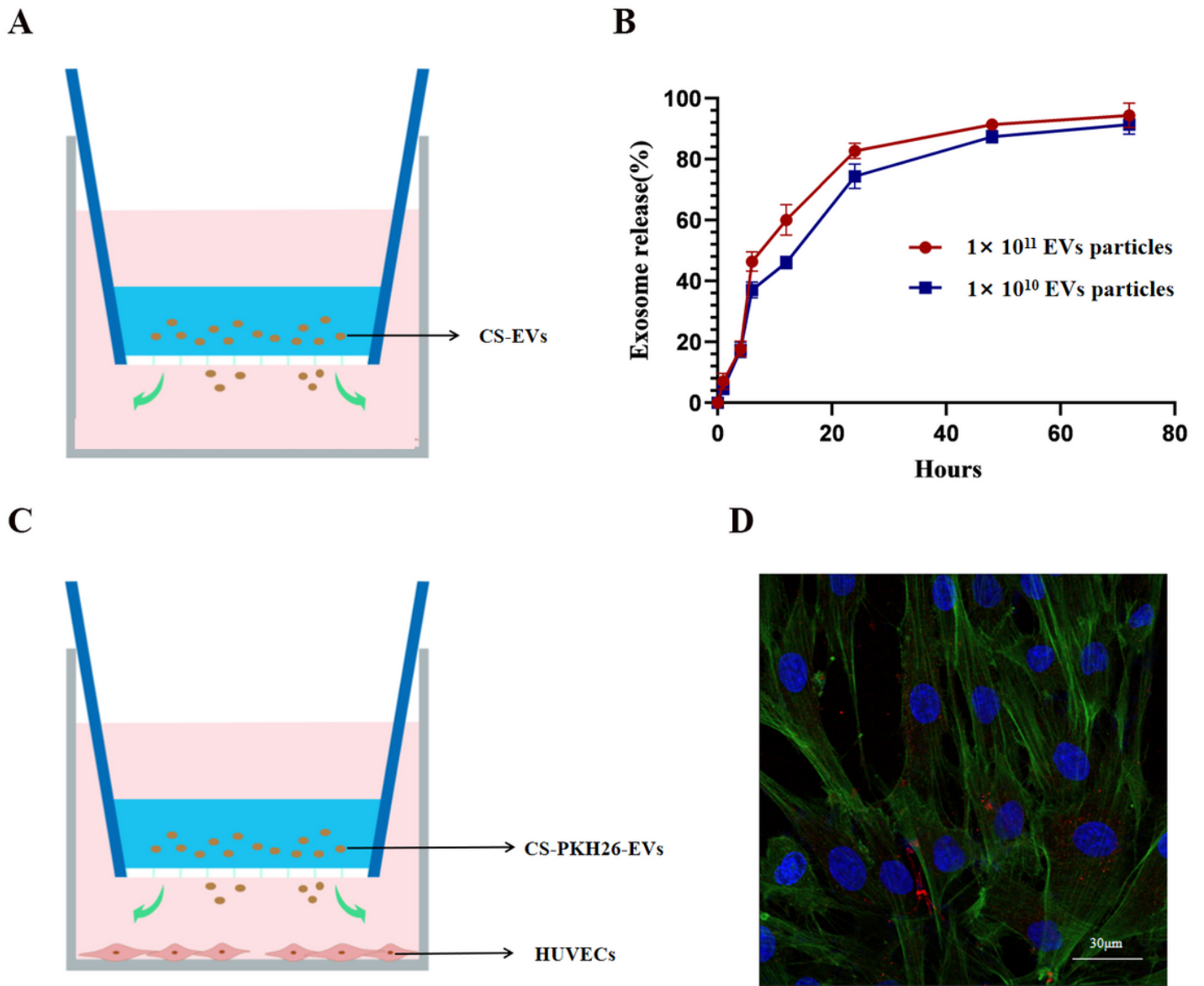


Figure 4

In vitro release and uptake behavior of EVs leaching from the CS-EVs. **A.** Schematic representation of CS-EVs in the upper Transwell chamber releasing EVs to the surroundings. **B.** The release profiles of EVs leaching from CS-EVs. **C.** Schematic representation of the CS-PKH26-EVs in the upper Transwell chamber releasing PKH26-EVs to the surroundings. **D.** The internalization of PKH26-labelled EVs by HUVECs.

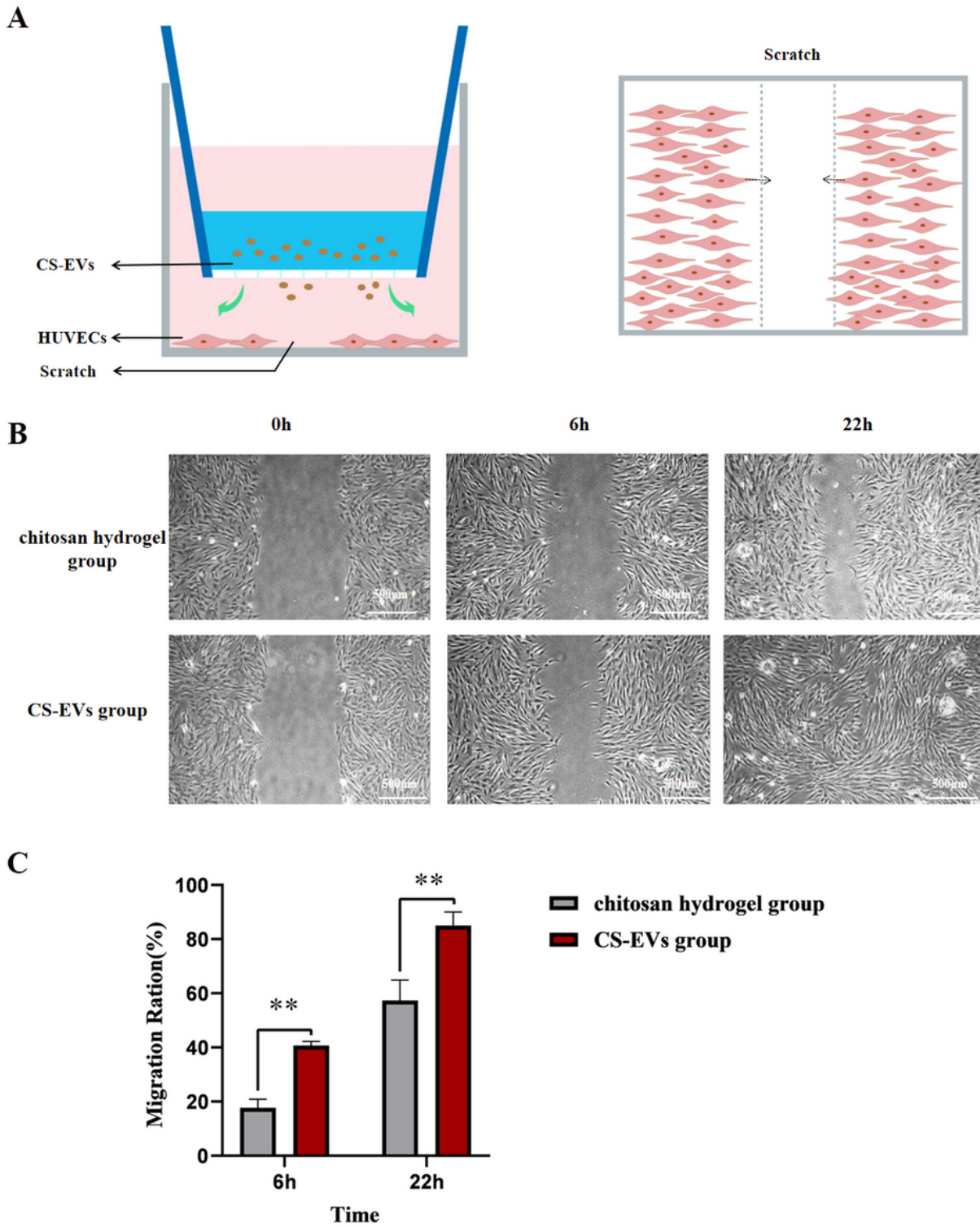


Figure 5

Enhanced migratory ability of CS-EVs in HUVEC. A. Schematic representation of migration tests. B. Images of cell migration in HUVEC at 6 h and 22 h. C. Quantification of cell migration rate in HUVEC. The asterisks (**) indicate $p < 0.01$.

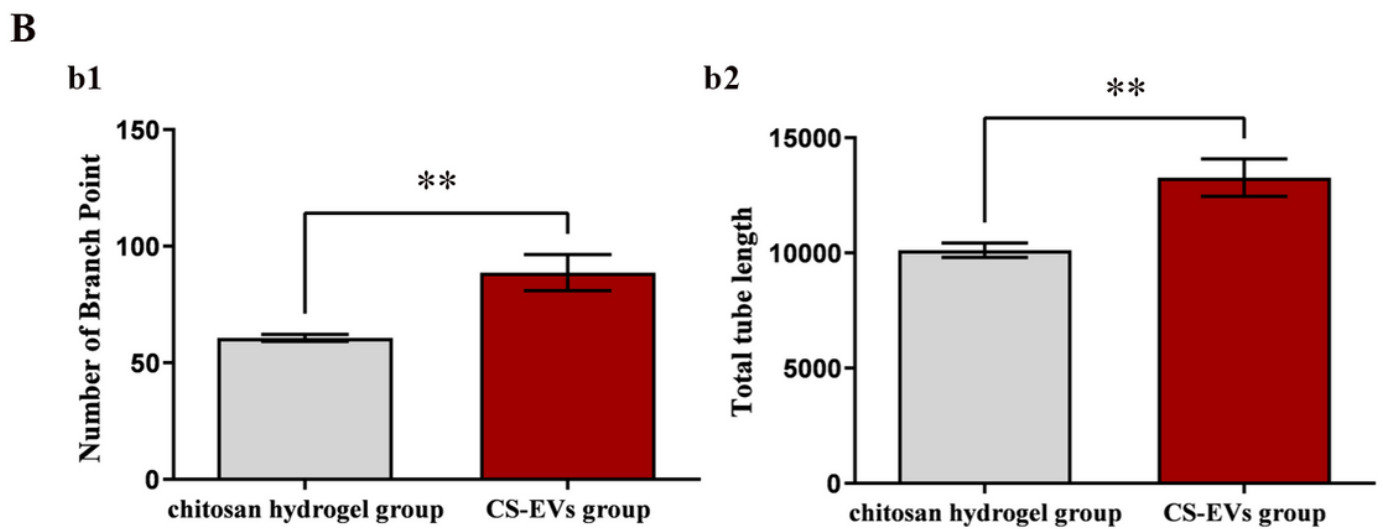
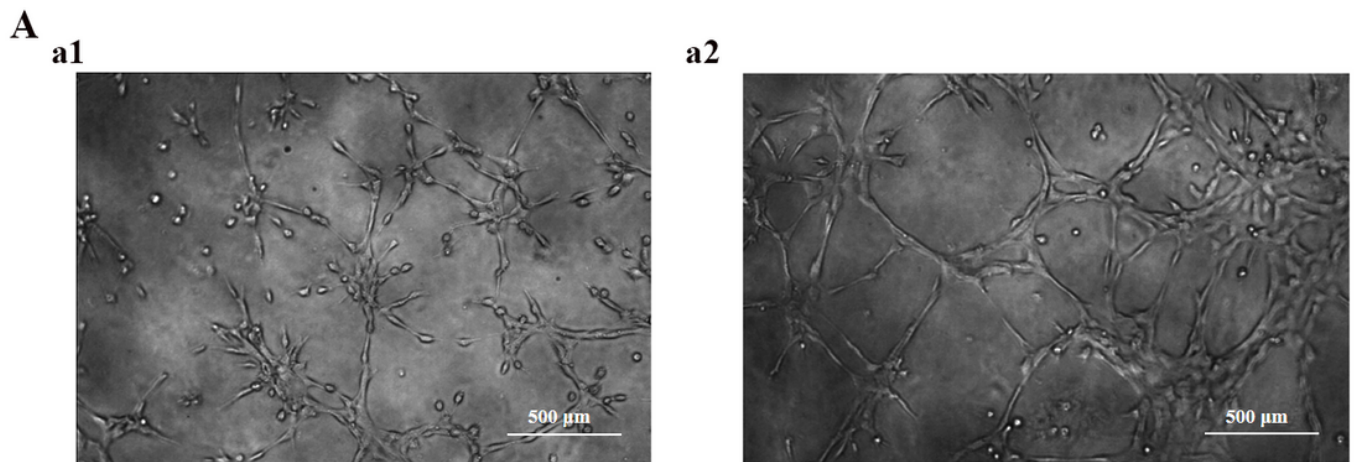


Figure 6

Tube formation assays. **A.** CS-EVs enhance the angiogenesis ability of HUVECs; a1. Chitosan hydrogel stimulates the tube formation ability of HUVECs; a2. CS-EVs stimulate the tube formation ability of HUVECs. **B.** Quantitative analysis of the angiogenic capacity of HUVECs. b1. Branch point number in both groups; b2. Total tube length in both groups. The asterisks (**) indicate $p < 0.01$.

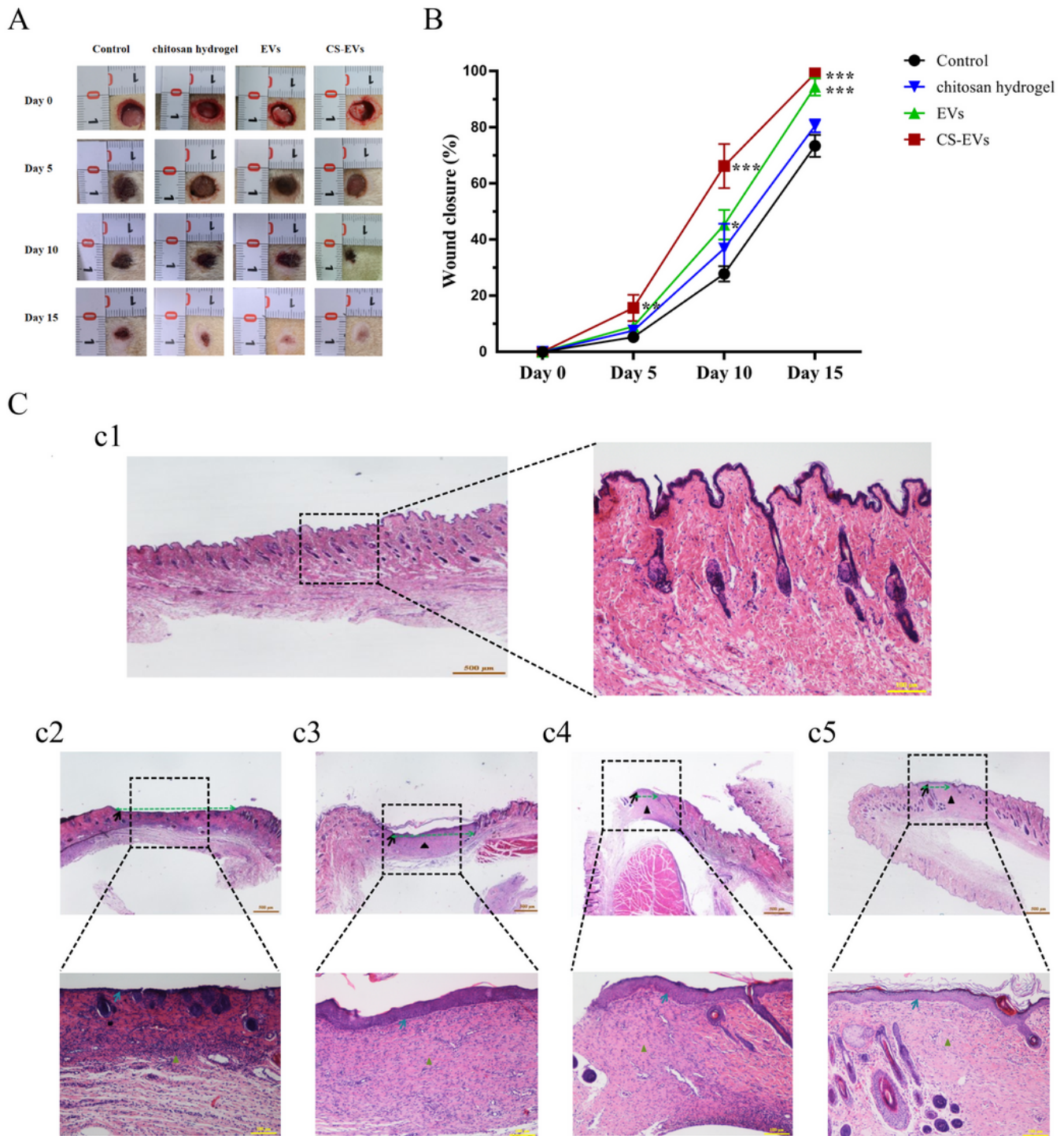


Figure 7

In vivo analysis of wound healing. **A.** The wounds were photographed on days 0, 5, 10, and 15. **B.** Quantitative analysis of the rates of wound healing. **C.** Histopathological analysis of wounds on day 15; c1. Control (normal skin); c2. PBS group; c3. Chitosan hydrogel group; c4. EVs group; c5. CS-EVs group. The asterisks (**) indicate $p < 0.01$ and (***) indicate $p < 0.001$.